Asian Journal of Chemistry; Vol. 34, No. 11 (2022), 2969-2974

ASIAN JOURNAL OF CHEMISTRY

https://doi.org/10.14233/ajchem.2022.23940


# Near White Emitting Host Sensitized $Dy^{3+}$ doped $GdPO_4$ Nanoparticles: Luminescence Studies

ELIZABETH CHINGANGBAM[1,2], N. YAIPHABA[2,*] and GANNGAM PHAOMEI[3]

[1]Department of Chemistry, Manipur University, Canchipur-795003, India
[2]Department of Chemistry, D.M. College of Science, Dhanamanjuri University, Imphal-795001, India
[3]Department of Chemistry and CoENSTds, Berhampur University, Berhampur-760007, India

*Corresponding author: Fax: +91 385 2450049; E-mail: ningombam.y@gmail.com

*Received*: 30 May 2022; *Accepted*: 22 September 2022; *Published online*: 19 October 2022; AJC-21015

Host sensitized $GdPO_4$ nanoparticles doped with $Dy^{3+}$ ions have been prepared by co-precipitation method with ethylene glycol as capping agent as well as solvent. The as-prepared samples exhibit crystalline monoclinic phase of $GdPO_4$. From the luminescence study, $^4F_{9/2}\rightarrow{}^6H_{15/2}$ of $Dy^{3+}$ is dominant over $^4F_{9/2}\rightarrow{}^6H_{13/2}$ transition indicating the occupation of inversion symmetry by $Dy^{3+}$ ions in the host lattice. The steady state luminescence shows effective energy transfer from gadolinium ($Gd^{3+}$) to dysprosium ($Dy^{3+}$) ions in the doped samples with optimum emission of $Dy^{3+}$ (2 at.%) doped sample. Decay lifetime values also decrease upon increasing $Dy^{3+}$ ion concentration on account of cross-relaxation concentration quenching effect. The emission colour of single phase as-prepared $Dy^{3+}$ doped $GdPO_4$ nanoparticles can be tuned from blue-violet to near white light by changing the excitation wavelength. Tunability of the light and white light emission are supported by Commission Internationale de l'Eclairage (CIE) chromaticity.

**Keywords: Co-precipitation, Monoclinic, Luminescence, Inversion symmetry, Energy transfer.**

## INTRODUCTION

Rare-earth (RE) doped nanoparticles are of great significance as display and lighting devices, solid state lighting (SSL), biological labelling, lasers, catalysis, bioimaging, sensing devices, *etc*. [1-4]. They have superior properties and wider applications owing to the quantum confinement effect, comparatively smaller size and larger surface-volume ratio than the micro-sized or macro-sized particles [5,6]. Rare-earth (RE) ions have shown narrow and sharp emission due to forbidden 4*f*-4*f* transition and hence serve as promising activators for many hosts.

Recently, lanthanide activated nanophosphors are being focussed for solid state lighting. Solid state lighting (SSL) has attracted a considerable attention because of its efficient luminous intensity, better reliability, longer lifetime, lower energy consumption than conventional incandescent and fluorescent lamps [7]. Generally, white light is generated by conversion of phosphor. For example, $Y_3Al_5O_{12}:Ce^{3+}$ pumped with blue light emitting diode (LED) is commercially used to generate white light [8]. Also, $Ba_2Gd_2Si_4O_{13}:Eu^{3+}$ (red phosphors) and $Ca_3Si_2O_4N_2:Eu^{2+}$ (green phosphors) are used to generate white light [9,10]. However, the manufacturing cost of white LEDs from such phosphor powder is generally high. One of the main reasons is that such phosphors are prepared at a high temperature of ~1300 ºC by solid state synthesis.

At present, the main focus of lanthanide activated nanophosphors is on the production of low-cost white emitting LEDs with high colour rendering index and high luminous efficacy. An alternative is the development of a single-phase white emitting phosphor doped with lanthanide ions that can be synthesized at low temperature by simple chemical methods. In this aspect, synthesis of lanthanide ion doped in different host materials like $YVO_4:Tm^{3+}/Eu^{3+}/Dy^{3+}$, $YPVO_4:Sm^{3+}/Dy^{3+}$, $YPO_4:Tb^{3+}/Eu^{3+}/Sr^{2+}$, *etc*. were reported [7,11,12]. Devi *et al.* [13] reported white light emitting $YP_{0.8}V_{0.2}O_4$ by controlled doping of $Sm^{3+}$ ions. Sharma & Singh *et al.* [14] showed that doping $Dy^{3+}$ ions in calcium molybdate can be used to obtain white light by the combination of blue and yellow white light. $Dy^{3+}$ doped $Ca_3Bi(PO_4)_3$ phosphor prepared by co-precipitation method serving as white light-emitter has also been reported [15]. In particular, $Dy^{3+}$ ion is one of the widely doped rare earth ions in various host matrices such as calcium tungstates, yttrium phosphates, gadolinium phosphates, *etc*. It exhibits

blue emission corresponding to $^4F_{9/2} \rightarrow {}^6H_{15/2}$ transition and $^4F_{9/2} \rightarrow {}^6H_{13/2}$ transition resulting in yellow emission [16]. Only the yellow emission is hypersensitive to the host environment. Hence, $Dy^{3+}$ doped nanomaterials in suitable hosts could serve as potential white light emitter under suitable environment and by tuning appropriate yellow to blue intensity ratio.

The present work deals with the synthesis of dysprosium doped gadolinium phosphate, $Gd_{1-x}Dy_xPO_4$ ($x$ = 0, 2, 5, 7, 10, 15 and 20 at.%) nanoparticles by co-precipitation method with ethylene glycol as capping agent as well as solvent. Its advantages are, it can be carried out in normal atmospheric conditions at low temperature of 160 ºC, requires less time, easy to perform, provides high yield and also enables uniform mixing of reactants [17-19]. The main reason for choosing $GdPO_4$ as host is because of its unique properties such as biocompatibility, less cytotoxicity, high thermal stability and a good potential for bioimaging [20,21]. Moreover, gadolinium has a strong absorption at 274 nm, which transfer its energy to the activator thereby improving luminescent properties. The luminescence properties, energy transfer and decay lifetime of the as-prepared samples are studied. Also, from the emission spectra, the chromaticity studies were also investigated.

## EXPERIMENTAL

$GdPO_4:Dy^{3+}$ (0, 2, 5, 7, 10, 15, 20 at.%) nanoparticles were prepared by a simple co-precipitation method in an ethylene glycol medium at a temperature of 160 ºC. Gadolinium oxide, dysprosium carbonate and ammonium dihydrogen phosphate, $NH_4H_2PO_4$ were used as sources of $Gd^{3+}$, $Dy^{3+}$ and $PO_4^{3-}$ ions, respectively.

For a typical preparation of 2 at.% $Dy^{3+}$ doped $GdPO_4$ sample, 0.5 g of $Gd_2O_3$ and 0.0142 g of $Dy_2(CO_3)_3$ were dissolved in 2 mL of conc. HCl. The chlorides of $Gd^{3+}$ and $Dy^{3+}$ so formed were mixed with 0.3238 g of $NH_4H_2PO_4$ and then dissolved in minimum amount of distilled water. To the reaction mixture, 50 mL of ethylene glycol was then added. The resulting solution was finally refluxed for 3 h by maintaining a temperature of 160 ºC and kept overnight. The precipitate formed was collected by centrifugation at 10000 rpm for 5 min. It was then washed 3 times with ethanol. The precipitate was finally dried in the oven at an ambient temperature of ~50 ºC and collected for future characterization.

**Characterization:** The X-ray diffraction (XRD) peaks of the as-prepared samples were recorded using a Philips Powder X-Ray Diffractometer (model PW 1071) with nickel filtered copper $K\alpha$ radiation. The infrared spectrum was characterized with a SHIMADZU (model 8400 S) spectrometer by making thin pellets with KBr. The excitation and emission spectra were measured at room temperature using a Hitachi F-4500 fluorescence spectrometer having excitation source 150 W xenon lamp. The decay life-time studies for $Dy^{3+}$ transitions were carried out using Edinburgh Instrument (model F920) with µs flash lamp as the excitation source.

## RESULTS AND DISCUSSION

**XRD study:** The XRD peaks of as-prepared $GdPO_4$ nanoparticles doped with different concentrations of $Dy^{3+}$ ions are shown in Fig. 1. All the peaks conform well to the monoclinic crystalline structure corresponding to JCPDS card no. 32-0386 with no additional peaks. The average crystallite sizes of as-prepared $GdPO_4:Dy^{3+}$ ($x$ = 2, 5, 7, 10, 15 at.%) nanoparticles calculated using Debye-Scherrer's formula ($d = 0.9\lambda/\beta\cos\theta$) ranges from 25 to 49 nm and agrees with TEM study reported earlier [22].

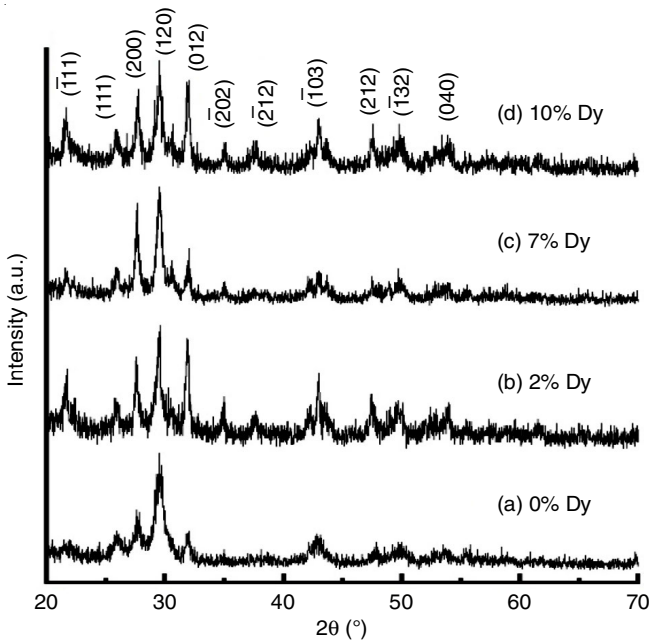


Fig. 1. XRD peaks of $GdPO_4$ nanoparticles doped with $Dy^{3+}$ ions (0, 2, 7, 10 at.%)

The lattice parameters, calculated unit cell volumes and the average crystallite sizes of the samples are given in Table-1. The unit cell volume of undoped $GdPO_4$ nanoparticle (279.81 $Å^3$) agrees well with that of the reference value (JCPDS card no. 32-0386). The unit cell volume decreases with increasing $Dy^{3+}$ ions concentration indicating the substitution of larger sized $Gd^{3+}$ ions (1.107 Å) by smaller sized $Dy^{3+}$ ions (1.083 Å) in the doped $GdPO_4$ samples [23]. The homogenous substitution of the plot of unit cell volume *versus* $Dy^{3+}$ concentration is shown in Fig. 2. The incorporation of $Tb^{3+}$ into $GdPO_4$ host lattice has already been discussed and reported elsewhere [22].

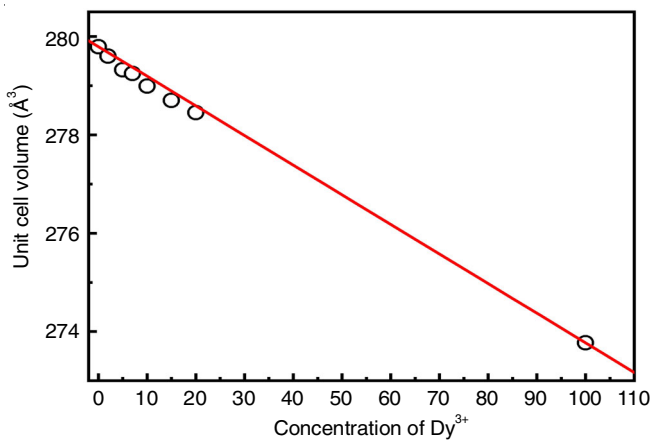


Fig. 2. Plot of unit cell volume ($Å^3$) *vs.* $Dy^{3+}$ concentration

TABLE-1
UNIT CELL VOLUME OF $GdPO_4$ NANOPARTICLES DOPED WITH $Dy^{3+}$ IONS (0, 2, 5, 7, 10, 15 at.%)

| Sample | Lattice parameters | | | | Crystallite size (nm) |
|---|---|---|---|---|---|
| | a (Å) | b (Å) | c (Å) | V (Å$^3$) | |
| JCPDS (32-0386) | 6.6525 | 6.8451 | 6.3342 | 279.86 | – |
| $GdPO_4:Dy^{3+}$ (0 at.%) | 6.6592 | 6.8316 | 6.3351 | 279.81 | 25 |
| $GdPO_4:Dy^{3+}$ (2 at.%) | 6.6632 | 6.8304 | 6.3372 | 279.72 | 35 |
| $GdPO_4:Dy^{3+}$ (5 at%) | 6.6402 | 6.8483 | 6.3367 | 279.50 | 49 |
| $GdPO_4:Dy^{3+}$ (7 at.%) | 6.6628 | 6.8622 | 6.3039 | 279.36 | 39 |
| $GdPO_4:Dy^{3+}$ (10 at.%) | 6.6376 | 6.8471 | 6.3322 | 279.18 | 34 |
| $GdPO_4:Dy^{3+}$ (15 at.%) | 6.6471 | 6.8318 | 6.3304 | 278.89 | 28 |

**IR study:** Fig. 3 shows the IR spectrum of 2 at.% doped $GdPO_4$ nanoparticle. The peaks at 551 and 627 cm$^{-1}$ assigned as $\nu_4$ mode is due to O-P-O asymmetric bending vibration of $PO_4^{3-}$ ions [24]. The P-O symmetric stretching vibration ($\nu_1$ mode) and the P-O asymmetric stretching vibration ($\nu_3$ mode) are observed at 966 and 1079 cm$^{-1}$, respectively [24]. The bending vibrations of $CH_2$ group of ethylene glycol molecule are 1397 and 1457 cm$^{-1}$ while the $CH_2$ stretching vibrations of ethylene glycol molecule are observed at 2882 and 2955 cm$^{-1}$ [25]. The peak observed at 2361 cm$^{-1}$ is due to the $CO_2$ molecule, which might be absorbed from the atmosphere on the surface of the nanoparticle [25]. The bending and stretching vibrations of OH group of ethylene glycol molecule are also observed at 1628 and 3346 cm$^{-1}$, respectively [22]. Thus, the IR spectrum confirms the presence of ethylene glycol molecules on the surface of the nanoparticles. This is particularly useful since they can be incorporated into polar media like poly(vinyl alcohol) polymer and find applications in optical devices [22].

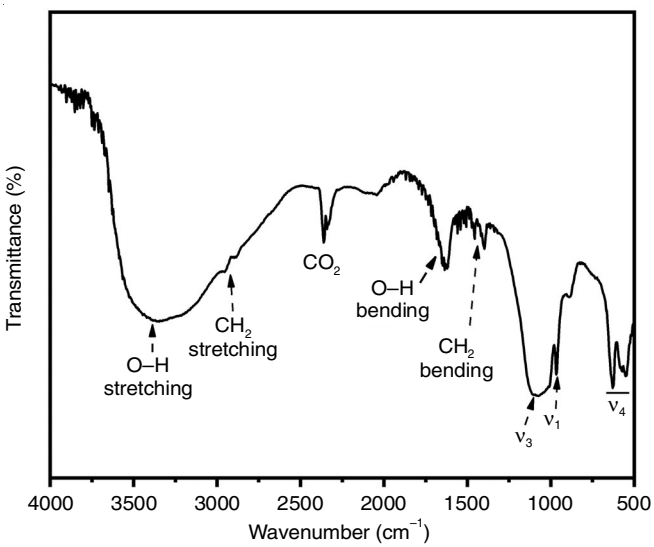


Fig. 3. IR spectrum of 2 at.% $Dy^{3+}$ doped $GdPO_4$ nanoparticle

**Excitation study:** The excitation spectra of $GdPO_4$ doped with $Dy^{3+}$ (2, 5, 7, 10, 15, 20 at.%) nanoparticles monitoring emission at 477 nm wavelength are shown in Fig. 4. The spectra consist of a sharp excitation peak at 275 nm and weaker peaks ranging from 300-400 nm. The sharp peak at 275 nm corresponds to $^8S_{7/2} \rightarrow {}^6I_J$ of $Gd^{3+}$ ions. Among the smaller peaks, the peak at 311 nm corresponds to the $^8S_{7/2} \rightarrow {}^6P_J$ transition of $Gd^{3+}$

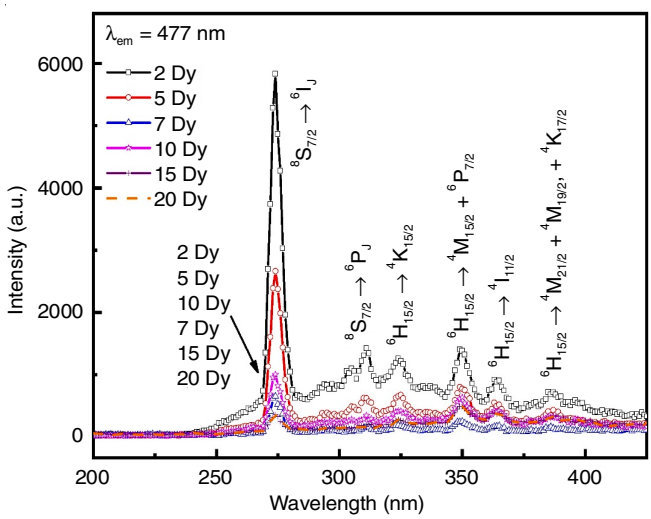


Fig. 4. Excitation spectra of $GdPO_4:Dy^{3+}$(2, 5, 7, 10, 15, 20 at.%) at 477 nm emission wavelength

ions [26]. Whereas the weaker peaks at 323, 350, 363 and 387 nm are the peaks due to $^6H_{15/2} \rightarrow {}^4K_{15/2}$ + $^6P_{3/2}$, $^6H_{15/2} \rightarrow {}^4M_{15/2}$ + $^6P_{7/2}$, $^6H_{15/2} \rightarrow {}^4I_{11/2}$ and $^6H_{15/2} \rightarrow {}^4M_{21/2}$ + $^4M_{19/2}$ + $^4K_{17/2}$ transitions of $Dy^{3+}$ ions, respectively [27,28]. Here, the presence of both $Gd^{3+}$ excitation peak and $Dy^{3+}$ excitation peak when monitored at $Dy^{3+}$ emission wavelength shows the presence of energy transfer from $Gd^{3+}$ to $Dy^{3+}$ ions [29,30] (discussed later). The most intense excitation peaks is obtained for 2 at.% $Dy^{3+}$ doped $GdPO_4$ sample while minimum intensity is observed for 20 at.% $Dy^{3+}$ doped sample.

**Emission study:** The emission spectra of $Dy^{3+}$ (2, 5, 7, 10, 15, 20 at.%) doped $GdPO_4$ nanoparticles at 275 nm excitation wavelength are shown in Fig. 5. Here, two strong emission peaks are observed at 477 nm (blue) and 572 nm (yellow). The blue emission corresponds to the magnetic dipole transition $^4F_{9/2} \rightarrow {}^6H_{15/2}$, while the yellow emission is due to the electric dipole transition $^4F_{9/2} \rightarrow {}^6H_{13/2}$ of $Dy^{3+}$ [31]. The magnetic dipole transition is less sensitive to the host environment while the electric dipole transition intensity is strongly influenced by the environment around $Dy^{3+}$. In general, when $Dy^{3+}$ ions are present at high symmetry, the blue emission dominates while the yellow emission dominates when $Dy^{3+}$ ions are present at low symmetry. From Fig. 5, the dominance of blue emission indicates the occupation of more $Dy^{3+}$ ions with an inversion centre in the host matrix [32]. The optimum emission peak is observed for 2 at.% $Dy^{3+}$ doped sample. The emission intensity further decreases with increasing $Dy^{3+}$ ion concentration due

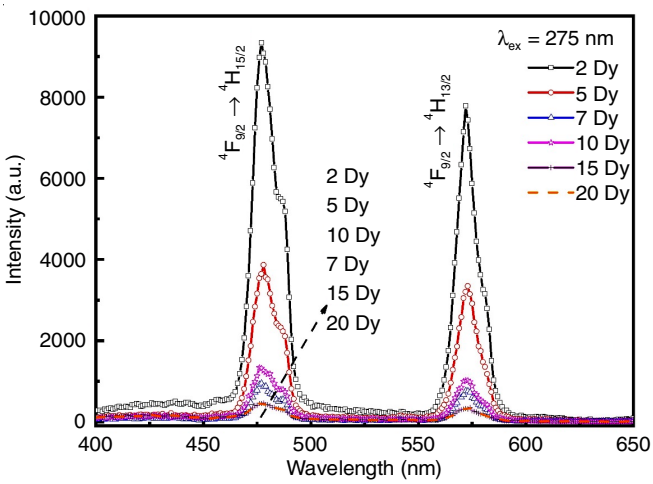


Fig. 5. Emission spectra of $GdPO_4$:$Dy^{3+}$ (2, 5, 7, 10, 15, 20 at.%) at 275 nm excitation wavelength

to the transfer of energy among $Dy^{3+}$ ions *i.e.* concentration quenching effect [33].

The emission peaks of $GdPO_4$:$Dy^{3+}$ (2 at.%) as-prepared sample studied at different excitation wavelengths 275, 311 and 350 nm are shown in Fig. 6. The spectra show similar spectral pattern with no additional peaks. The most intense spectrum is observed at 275 nm excitation, which corresponds to $^8S_{7/2} \rightarrow {}^6I_{11/2}$ of $Gd^{3+}$ ions (host excitation). While the direct excitation of the activator, $Dy^{3+}$ (350 nm, $^6H_{15/2} \rightarrow {}^4M_{15/2} + {}^6P_{7/2}$) exhibits least intense emission spectra. This may be due to the probable energy transfer mechanism taking place in the prepared samples from host to activator *i.e.* $Gd^{3+}$ to $Dy^{3+}$ ion. From the spectra, of the two host transitions, the transition at 275 nm shows better energy transfer than that at 311 nm ($^8S_{7/2} \rightarrow {}^6P_{11/2}$) transition. A schematic diagram for energy transfer is shown in Fig. 7. There is sufficient energy transfer from the sensitizer *i.e.* $^8S_{7/2} \rightarrow {}^6I_J$ (275 nm) and $^8S_{7/2} \rightarrow {}^6P_J$ transitions (311 nm) of $Gd^{3+}$ ions to the different excited states of $Dy^{3+}$ ions. Then, it undergoes internal conversion to the lowest excited state $^4F_{9/2}$ (Kasha's Rule) [34] from which it further undergoes radiative blue and yellow emission corresponding to $^4F_{9/2} \rightarrow {}^6H_{15/2}$ and $^4F_{9/2} \rightarrow {}^6H_{13/2}$ transition at 477 and 572 nm, respectively.

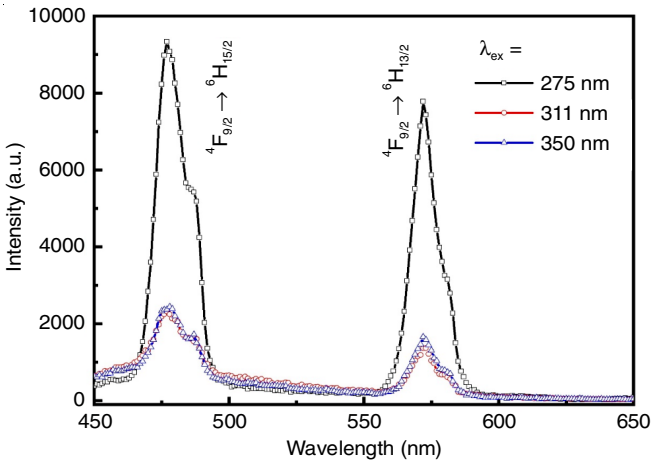


Fig. 6. Emission spectra of $GdPO_4$:$Dy^{3+}$(2 at.%) at $\lambda_{ex}$ = 275, 311 and 350 nm wavelength

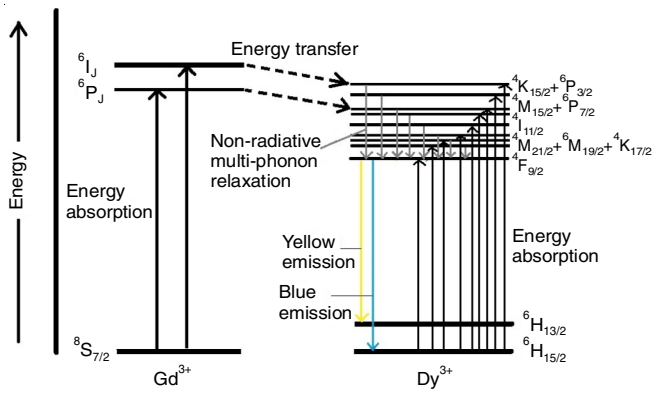


Fig. 7. Schematic diagram showing energy transfer from $Gd^{3+}$ to $Dy^{3+}$ ions

The integrated area for the transition $^8S_{7/2} \rightarrow {}^6I_J$ studied as a function of $Dy^{3+}$ concentration for all the $Dy^{3+}$ doped samples is shown in Fig. 8. It is observed that the emission intensity decreases with increase in concentration. The decrease in emission intensity with increase in $Dy^{3+}$ concentration is attributed to the dissipation of energy among the nearby $Dy^{3+}$ ions [33].

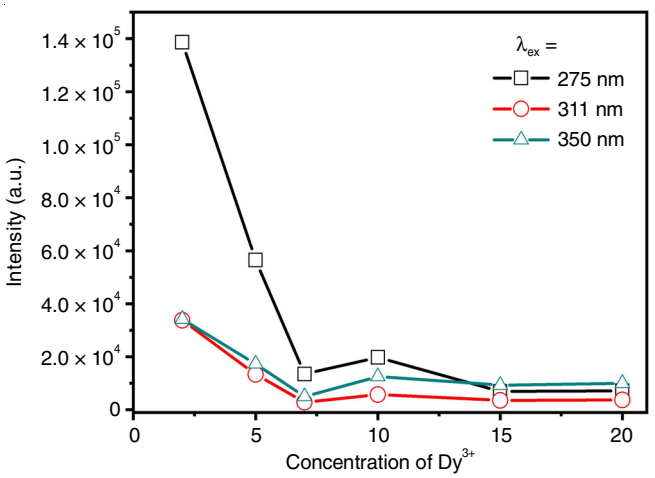


Fig. 8. Integrated area (intensity) under the $^8S_{7/2} \rightarrow {}^6I_J$ peak *versus* $Dy^{3+}$ concentration in $Dy^{3+}$ doped $GdPO_4$ nanoparticles at 275, 311 and 350 nm excitation wavelengths

**Lifetime study:** The decay lifetime of the as-prepared $Dy^{3+}$ doped $GdPO_4$ samples at 275 nm excitation wavelength and monitoring emission at 572 nm wavelength are shown in Fig. 9. The decay curve is analyzed by fitting with biexponential equations [35] expressed as:

$$I(t) = I_0 + I_1 \exp^{(-t/t1)} + I_2 \exp^{(-t/t2)} \quad (1)$$

where I(t) and $I_0$ represents the luminescence intensities at time t and 0, respectively, $I_1$ and $I_2$ are the intensities at different time intervals $t_1$ and $t_2$ respectively, $\tau_1$ and $\tau_2$ are the corresponding lifetimes.

Table-2 gives the average lifetime ($\tau_{av}$) of as-prepared $GdPO_4$:$Dy^{3+}$ (2, 5, 7, 10, 15, 20 at.%) samples calculated using eqn. 2:

$$\tau_{av} = \frac{(I_1\tau_1^2 + I_2\tau_2^2)}{(I_1\tau_1 + I_2\tau_2)} \quad (2)$$

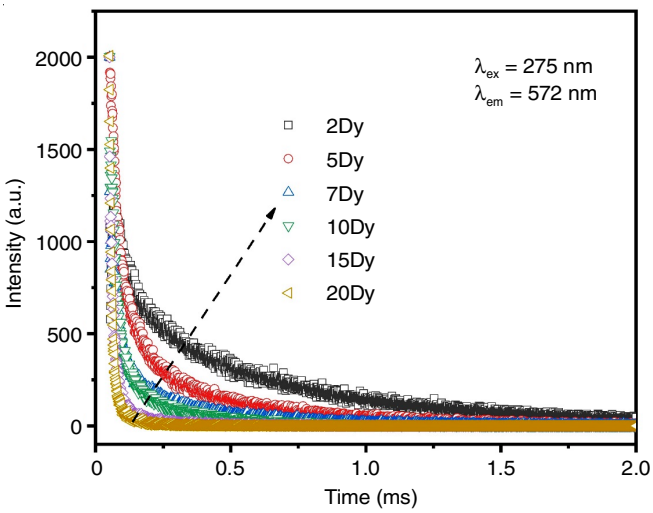


Fig. 9. Emission decay curve for $GdPO_4:Dy^{3+}$ (2, 5, 7, 10, 15, 20 at.%) at 275 nm excitation and monitoring emission at 572 nm wavelength

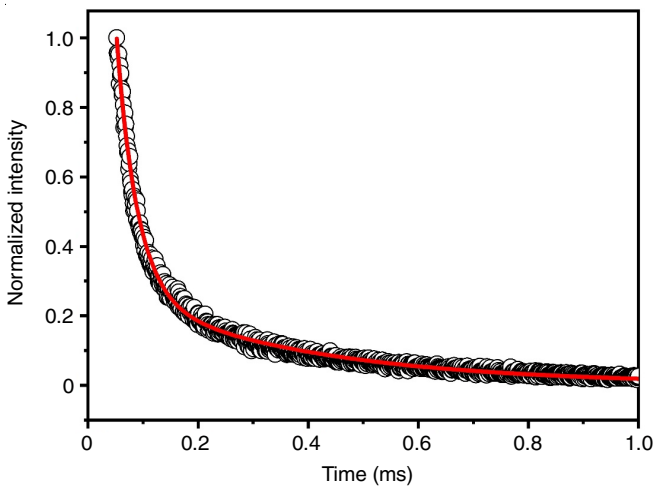


Fig. 10. Decay curve for $^4F_{9/2}$ level of $Dy^{3+}$ (5 at.%) doped $GdPO_4$ nanoparticle at 275 nm excitation wavelength and monitoring emission at 572 nm fitted biexponentially

TABLE-2
BI-EXPONENTIAL AVERAGE LIFETIME VALUES (ms) OF AS-PREPARED $GdPO_4:Dy^{3+}$ (2, 5, 7, 10, 15, 20 at.%) AT $\lambda_{ex}$ = 275 nm AND $\lambda_{em}$ = 572 nm

| $Dy^{3+}$ concentration (at.%) | $t_1$ (ms) | $t_2$ (ms) | $t_{av}$ (ms) |
|---|---|---|---|
| 2 | 0.11024 | 0.6565 | 0.55177 |
| 5 | 0.03772 | 0.34457 | 0.18639 |
| 7 | 0.02851 | 0.28599 | 0.12270 |
| 10 | 0.02464 | 0.21707 | 0.06687 |
| 15 | 0.01171 | 0.08397 | 0.01336 |
| 20 | 0.00338 | 0.01230 | 0.00483 |

The decay plots of all the prepared samples fit well with the biexponential function. A typical biexponential fit studied at 275 nm excitation wavelength and monitoring emission at 572 nm for 5 at.% $Dy^{3+}$ doped sample having $R^2$ = 0.99574 and other parameters are shown in Fig. 10.

The possibilities for the biexponential decay observed are (i) lanthanide ions near the surface have differing non-radiative probability compared with the core of the particles [35]; (ii) non-uniform distribution of dopant ions in the host [35]; and (iii) energy transfer from the host (sensitizer) to the activator [36].

The fitting of decay curve of the samples with biexponential function shows the energy transfer mechanism in the prepared samples *i.e.* from the host $Gd^{3+}$ ion to the activator $Dy^{3+}$ ion. Also, the regular decrease in decay lifetime upon increase in $Dy^{3+}$ concentration observed at 275 nm excitation and monitoring emission at 572 nm (Fig. 9) is due to the concentration quenching effect of $Dy^{3+}$ ions [33].

**CIE chromaticity study:** The Commission Internationale de l'Eclairage (CIE) chromaticity diagram of $GdPO_4:Dy^{3+}$(2, 5, 7, 10 at.%) nanoparticles at excitation wavelengths 275, 311 and 350 nm are shown in Fig. 11. Upon excitation at 275 nm, the CIE coordinates of $Dy^{3+}$ (2, 5, 7, 10 at.%) doped samples are close to that of ideal white light ($x$ = 0.33 and $y$ = 0.33). However, doped samples studied at 311 and 350 nm excitation wavelengths show CIE coordinates in the near blue region (Table-3). Luwang *et al.* [11] also reported that $YVO_4:Dy^{3+}$

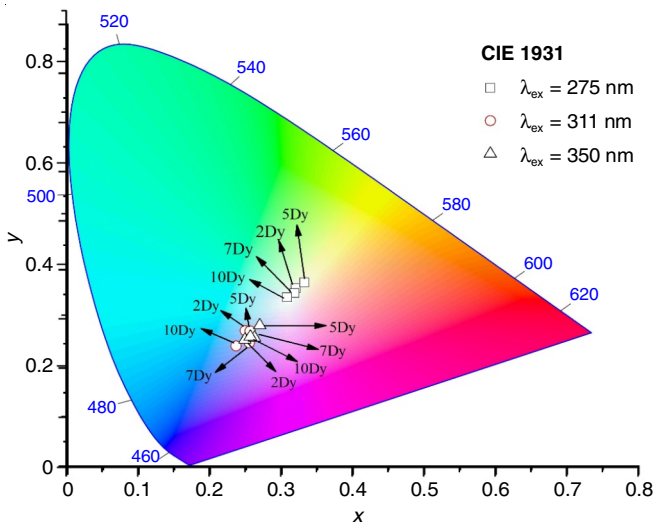


Fig. 11. Chromaticity diagram of $GdPO_4$ nanoparticles doped with $Dy^{3+}$(2, 5, 7, 10 at.%) at excitation wavelengths (275, 311 and 350 nm)

TABLE-3
CIE COLOUR CO-ORDINATES OF $GdPO_4:Dy^{3+}$ (2, 5, 7, 10, 15, 20 at.%) AT $\lambda_{ex}$ = 275, 311 AND 350 nm

| $Dy^{3+}$ concentration (at.%) | $\lambda_{ex}$ = 275 nm | | $\lambda_{ex}$ = 311 nm | | $\lambda_{ex}$ = 350 nm | |
|---|---|---|---|---|---|---|
| | $x$ | $y$ | $x$ | $y$ | $X$ | $y$ |
| 2 | 0.31982 | 0.36257 | 0.24894 | 0.27588 | 0.24839 | 0.25804 |
| 5 | 0.33186 | 0.37428 | 0.25589 | 0.27539 | 0.26922 | 0.28686 |
| 7 | 0.31805 | 0.35271 | 0.25482 | 0.25100 | 0.26190 | 0.26208 |
| 10 | 0.30727 | 0.34423 | 0.23601 | 0.24489 | 0.25592 | 0.26395 |
| 15 | 0.27980 | 0.28983 | 0.21861 | 0.19695 | 0.24550 | 0.24395 |
| 20 | 0.29190 | 0.31062 | 0.23454 | 0.22011 | 0.25445 | 0.25172 |

coated with silica after annealing at 500 ºC shows near white light emission with CIE coordinates $x = 0.35$ and $y = 0.38$ [11]. Thus, by monitoring the samples at appropriate excitation wavelength and by controlling the concentration of dopant ion ($Dy^{3+}$), the doped nanoparticles could serve as a good potential for obtaining white light LEDs.

## Conclusion

The $Dy^{3+}$ doped $GdPO_4$ nanoparticles was prepared by co-precipitation method in an ethylene glycol medium as capping agent at 160 ºC. The incorporation of $Dy^{3+}$ ions into the monoclinic $GdPO_4$ matrix was confirmed by XRD studies. From luminescence studies, the strong absorption peaks of $Gd^{3+}$ ions act as a sensitizer to the activator, $Dy^{3+}$ ions. The dominance of magnetic dipole transition over the electric dipole transition shows the occupation of symmetric environment by $Dy^{3+}$ ions in the as-prepared $GdPO_4$ samples. From the emission spectra, maximum intensity was observed for 2 at.% $Dy^{3+}$ doped sample, which decreases with increase in concentration of $Dy^{3+}$ ions due to the concentration quenching. The decay lifetime values of $Dy^{3+}$ decrease from 551 µs (2 at.%) to 4 µs (20 at.%). The tunability of the light emission from blue (311 nm, 350 nm) to near white (275 nm) is supported by CIE chromaticity. This could find potential applications towards the development of white light emitting pcLEDs for solid state lighting (SSL).

## ACKNOWLEDGEMENTS

The authors acknowledge UGC, New Delhi and Manipur University, Canchipur, India for providing the financial support.

## CONFLICT OF INTEREST

The authors declare that there is no conflict of interests regarding the publication of this article.

## REFERENCES

1. T. Jüstel, H. Nikol and C. Ronda, *Angew. Chem. Int. Ed. Engl.*, **37**, 3084 (1998); https://doi.org/10.1002/(SICI)1521-3773(19981204)37:22<3084::AID-ANIE3084>3.0.CO;2-W
2. A. Gautam and F.C.J.M. van Veggel, *Chem. Mater.*, **23**, 4817 (2011); https://doi.org/10.1021/cm202139u
3. J.Y. Park, M.J. Baek, E.S. Choi, S. Woo, J.H. Kim, T.J. Kim, J.C. Jung, K.S. Chae, Y. Chang and G.H. Lee, *ACS Nano*, **3**, 3663 (2009); https://doi.org/10.1021/nn900761s
4. F. Zhang and S.S. Wong, *ACS Nano*, **4**, 99 (2010); https://doi.org/10.1021/nn901057y
5. S. Mourdikoudis, R.M. Pallares and N.T.K. Thanh, *Nanoscale*, **10**, 12871 (2018); https://doi.org/10.1039/C8NR02278J
6. A.P. Alivisatos, *Science*, **271**, 933 (1996); https://doi.org/10.1126/science.271.5251.933
7. N.S. Singh, N.K. Sahu and D. Bahadur, *J. Mater. Chem. C Mater. Opt. Electron. Devices*, **2**, 548 (2014); https://doi.org/10.1039/C3TC31586J
8. D. Haranath, H. Chander, P. Sharma and S. Singh, *App. Phys. Lett.*, **89**, 173118 (2006); https://doi.org/10.1063/1.2367657
9. H. Guo, H. Zhang, R.F. Wei, M.D. Zheng and L.H. Zhang, *Opt. Express*, **19(S2)**, A201 (2011); https://doi.org/10.1364/OE.19.00A201
10. Y.C. Chiu, C.H. Huang, T.J. Lee, W.R. Liu, Y.T. Yeh, S.M. Jang and R.S. Liu, *Opt. Express*, **19(S3)**, A331 (2011); https://doi.org/10.1364/OE.19.00A331
11. M.N. Luwang, R.S. Ningthoujam, S.K. Srivastava and R.K. Vatsa, *J. Mater. Chem.*, **21**, 5326 (2011); https://doi.org/10.1039/c0jm03470c
12. W. Tang, M. Wang, X. Meng and W. Lin, *Opt. Mater.*, **54**, 120 (2016); https://doi.org/10.1016/j.optmat.2016.02.018
13. N.S. Singh, R. Wangkhem, T. Yaba, S. Devi, M.N. Luwang, N. Yaiphaba, H.S. Devi and Th.D. Singh, *J. Alloys Compd.*, **726**, 1161 (2017); https://doi.org/10.1016/j.jallcom.2017.08.099
14. K.G. Sharma and N.R. Singh, *New J. Chem.*, **37**, 2784 (2013); https://doi.org/10.1039/c3nj00155e
15. M.K. Sahu and J. Mula, *J. Am. Ceram. Soc.*, **102**, 6087 (2019); https://doi.org/10.1111/jace.16479
16. T. Yaba, R. Wangkhem and N.S. Singh, *J. Fluoresc.*, **29**, 435 (2019); https://doi.org/10.1007/s10895-019-02352-w
17. D. Yu, Y. Liang, M. Zhang, M. Tong, Q. Wang, J. Zhao, J. Wu, G. Li and C. Yan, *J. Mater. Sci. Mater. Electron.*, **25**, 3526 (2014); https://doi.org/10.1007/s10854-014-2050-8
18. N. Jain, N. Marwaha, R. Verma, B.K. Gupta and A.K. Srivastava, *RSC Adv.*, **6**, 4960 (2016); https://doi.org/10.1039/C5RA21150F
19. X. Li, T. OdoomWubah, Z. Chen, B. Zheng and J. Huang, *Ceram. Int.*, **40**, 16317 (2014); https://doi.org/10.1016/j.ceramint.2014.07.070
20. M.F. Dumont, C. Baligand, Y. Li, E.S. Knowles, M.W. Meisel, G.A. Walter and D.R. Talham, *Bioconjugate Chem.*, **23**, 951 (2012); https://doi.org/10.1021/bc200553h
21. Q. Yang, X. Li, Z. Xue, Y. Li, M. Jiang and S. Zeng, *RSC Adv.*, **8**, 12832 (2018); https://doi.org/10.1039/C7RA12864A
22. N. Yaiphaba, R.S. Ningthoujam, N.R. Singh and R.K. Vatsa, *Eur. J. Inorg. Chem.*, **2010**, 2682 (2010); https://doi.org/10.1002/ejic.200900968
23. R.D. Shannon, *Acta Crystallogr. A*, **32**, 751 (1976); https://doi.org/10.1107/S0567739476001551
24. L. Macalik, P. Tomaszewski, A. Pelczarska, I. Szczygiel, P. Solarz, P. Godlewska, M. Sobczyk and J. Hanuza, *J. Alloys Compd.*, **509**, 7458 (2011); https://doi.org/10.1016/j.jallcom.2011.04.077
25. R.S. Ningthoujam, V. Sudarsan and S.K. Kulshreshtha, *J. Lumin.*, **127**, 747 (2007); https://doi.org/10.1016/j.jlumin.2007.05.004
26. G.S.R. Raju, J.Y. Park, H.C. Jung, B.K. Moon, J.H. Jeong and J.H. Kim, *J. Electrochem. Soc.*, **158**, J20 (2011); https://doi.org/10.1149/1.3511786
27. W.C. Lü, H. Zhou, G.T. Chen, J.F. Li, Z.J. Zhu, Z.Y. You and C.Y. Tu, *J. Phys. Chem. C*, **113**, 3844 (2009); https://doi.org/10.1021/jp8082369
28. H. Zhang, X. Fu, S. Niu and Q. Xin, *J. Alloys Compd.*, **457**, 61 (2008); https://doi.org/10.1016/j.jallcom.2007.02.134
29. E.V.D. Van Loef, P. Dorenbos, C.W.E. Van Eijk, K.W. Krämer and H.U. Güdel, *Opt. Commun.*, **189**, 297 (2001); https://doi.org/10.1016/S0030-4018(01)01039-2
30. Z.L. Wang, J.H. Hao and H.L.W. Chan, *J. Electrochem. Soc.*, **157**, J315 (2010); https://doi.org/10.1149/1.3467789
31. M. Ferhi, S. Toumi, K. Horchani-Naifer and M. Ferid, *J. Alloys Compd.*, **714**, 144 (2017); https://doi.org/10.1016/j.jallcom.2017.04.193
32. C. Cao, H.K. Yang, B.K. Moon, B.C. Choi and J.H. Jeong, *J. Electrochem. Soc.*, **158**, J6 (2011); https://doi.org/10.1149/1.3517458
33. Q. Su, J. Lin and B. Li, *J. Alloys Compd.*, **225**, 120 (1995); https://doi.org/10.1016/0925-8388(94)07020-2
34. M. Kasha, *Discuss. Faraday Soc.*, **9**, 14 (1950); https://doi.org/10.1039/df9500900014
35. J.W. Stouwdam and F.C.J.M. van Veggel, *Nano Lett.*, **2**, 733 (2002); https://doi.org/10.1021/nl025562q
36. M. Yu, J. Lin and J. Fang, *Chem. Mater.*, **17**, 1783 (2005); https://doi.org/10.1021/cm0479537